

Correct patient centering increases image quality without concomitant increase of radiation dose during adult intracranial computed tomography

Al Mohiy H^{1*}; Emad Alasar 2* and Charbel Saade ^{3*}

¹⁻²Department of Radiological Science, King Khalid University, Abha, Saudi Arabia.

^{3*}Department of Diagnostic Radiology, American University of Beirut Medical Center, Lebanon

Abstract

Purpose: To evaluate the impact of patient centering and radiation dose during intracranial computed tomography (ICT) on quantitative and qualitative image quality.

Materials and Methods: 500 consecutive patients who underwent ICT were retrospectively reviewed using a 128-slice CT scanner (Definition AS+, Siemens, Germany). Patients were subjected in equal numbers to one of two positioning protocols: Group A, poorly centered; and Group B, involved accurate centering prior to imaging. Gray-white matter (GWM) conspicuity, contrast-to-noise (CNR), and signal-to-noise (SNR) in each group were calculated. Qualitative image quality in terms of GWM differentiation, distinctness of posterior fossa contents, and overall diagnostic acceptability were evaluated by two neuroradiologists. The dose length product (DLP), CNR, SNR, and noise were measured between each group and data generated were compared using Mann-Whitney U non-parametric statistics. Visual grading characteristic (VGC) and kappa analyses were performed.

Results: The mean noise index was significantly lower in group B (2.61 ± 0.29) compared to A (2.66 ± 0.21) ($p < 0.02$). The mean attenuation of GWM, SNR, and CNR in the frontal lobe (A; $1:0.77, 0.84, 8.70 \pm 1.36$ and B; $1:0.65, 0.85, 15.32 \pm 1.21$) ($p < 0.02$), occipital lobe (A; $1:1.10, 1.18, 10.79 \pm 2.11$, and B; $1:0.94, 0.64, 14.41 \pm 3.09$) ($p < 0.04$), and cerebellum (A; $1:0.79, 0.90, 12.56 \pm 4.08$ and B; $1:0.82, 0.87, 14.07 \pm 2.28$) ($p < 0.04$) were significantly higher in group B compared to A, while the globus pallidus, caudate nucleus, and optic track in the basal ganglia demonstrated no difference in each group ($p > 0.05$). Mean DLP demonstrated no significance between each group (A: 1312.03 ± 133.92 , B: 1298.11 ± 130.61). The qualitative analyses demonstrated significant increases in VGC for each reader ($p < 0.02$) and inter-observer agreement was significantly increased in protocol B ($k = 0.81$) compared to A ($k = 0.62$).

Conclusion: Correct patient centering increases the CNR and SNR in both GWM in the left and right hemispheres of the brain during ICT.

Introduction

Computed tomography (CT) has become the mainstream tool in the diagnosis of intracranial head trauma. Its high speed and sub-millimeter spatial resolution has enabled this technology to be widely available in the emergency setting its use has increased sharply. However, with this rapid technological advance, the increased awareness of radiation exposure caused by medical imaging soon demonstrated an association with an increase in lifetime cancer risk [1–3].

Radiographers and radiologists are responsible for the administration of radiation dose following the as low as reasonably achievable (ALARA) principle. Radiographers are required to optimize CT parameters to produce optimal image quality during intracranial CT. Diagnostic reference level (DRL) is one of the references for optimizing radiation exposure. DRL has been used in medical imaging to indicate whether, in routine conditions, the patient dose of administered activity from a specific procedure is unusually high or low for that particular procedure [4]. DRL studies in adults [5–10] and pediatric [5, 10–13] populations have been widely reported. For both adult and pediatric imaging, optimal centering requires the head to be positioned at the iso-center of the gantry so as the tube rotates, the photons reaching the detector are uniform in nature providing uniform image quality on both sides of the brain hemisphere. However, a recent study [14] revealed that skin surface dose penalty of up to 140% with a mean dose penalty of 33% assuming that tube current is increased to compensate for the increased noise due to off-centering has resulted in poor image quality.

The radiologist's responsibility [7–12, 15, 16] is to determine the following: whether optimal CT has been performed; optimal gray-white matter (GWM) differentiation; proper cupping correction; good soft tissue discrimination; accurate, reliable HU calibration; high

spatial resolution and modulation transfer function and artifact-free posterior fossa and skull base.

The aggressive reduction of radiation dose may potentially result in substantial loss of image quality—such as GWM, increased signal-to-noise ratio (SNR), and reduced contrast-to-noise ratio (CNR) —highlighting the need for radiologists and technologists to optimize CT protocols in an effort to balance image quality and radiation dose [17]. Image quality differences during neuroradiological applications differ immensely. Most of the previously published papers have considered qualitative image quality [18]. Additionally, age, gender, and head diameter (HD) may be related to differences in cranial bone density, which can potentially affect the visualization of GWM when employing tube current modulation. The aims of this study were to evaluate the radiation dose of adult head CT examinations and the impact of patient centering of the same (performed at three different radiologic sites at the same institution) with quantitative and qualitative image, performed with conventional, commercially available multiple detector computed tomography (MDCT) equipment.

Materials and Methods

Study population

The institutional review board approved this study and written informed consent was waived since all studies were clinically indicated and patient data were evaluated anonymously. Between February 2013 and January 2014, 500 consecutive patients were retrospectively reviewed (mean age 77 ± 11.2 years, range 55–99 years, 249 male, 251 female) and included in this study (Table 1). Patient demographics were equally distributed:

Group A, poorly centered; and Group B, involved accurate centering prior to imaging.

Patients were referred from the requesting physician for a head CT after clinical assessment.

Table 1: Patient demographics

Parameter	
Male	249
Female	251
Age (years)*	77 ± 11.2
Height (cm)*	171 ± 12
Weight (kg)*	78 ± 9
BMI (kg/m ²)	25.6 ± 5.5

Note – Data are mean ± standard deviation

CT data acquisition

All CT examinations were obtained using a 128-slice single-source CT scanner (Siemens definition AS+, Siemens, Germany). Image acquisition parameters of the standard protocol included a collimation of 40 × 0.6 mm (acquisition slice thickness 0.75 mm), pitch of 0.55, rotation time of 1.0 s, tube voltage of 120 kV, and tube current of 320 mA s.

CT data reconstruction

Head CT examinations in both study groups were reconstructed using manufacture-based mathematical algorithms in the filtered back projection (FBP) mode. The reconstruction algorithm was used as a standard in both studies in order not to place bias at quantitative and qualitative image assessment. Reconstruction parameters in each group employed H30s + medium smooth convolution kernel, a slice-thickness of 4 mm with 4 mm increment and a display field-of-view appropriate to head size.

Table 2: Scanner and reconstruction parameters

	Protocol
Scanner Parameters	
kVp	120
Rotation time (sec)	0.4
Pitch	0.889:1
mA (modulation)	200
Direction/Range	Caudocranial
Reconstruction Parameters	
Reconstruction Type	FBP
Slice Thickness (mm)	256 x 0.625
Reconstruction Interval (mm)	0.5
Field Of View (mm)	250 x 250
Window Width and Level	36 : 80

Dose measurements

The volume CT dose index ($CTDI_{vol}$) and dose length product (DLP) were recorded for every CT examination from the manufacturers dose report summary. Effective dose (mSv) was estimated by multiplying DLP with a constant region-specific conversion co-efficient of 0.0021 mSv/ (mGy × cm) (19).

Patient centering

Patient centering was subjectively determined by the deviation from the midsagittal centerline on the image relative to the head holder, which is the center of the field of view (FOV). Group A patients were categorized when the superior sagittal sinus was not in the center of the field of view (greater than 2 cm deviation in each direction) and head cradle (determined as the center of the scan FOV by the manufacturer) (Figure 1b). Group B patients were exactly in the center of the FOV and cradle (Figure 1a).

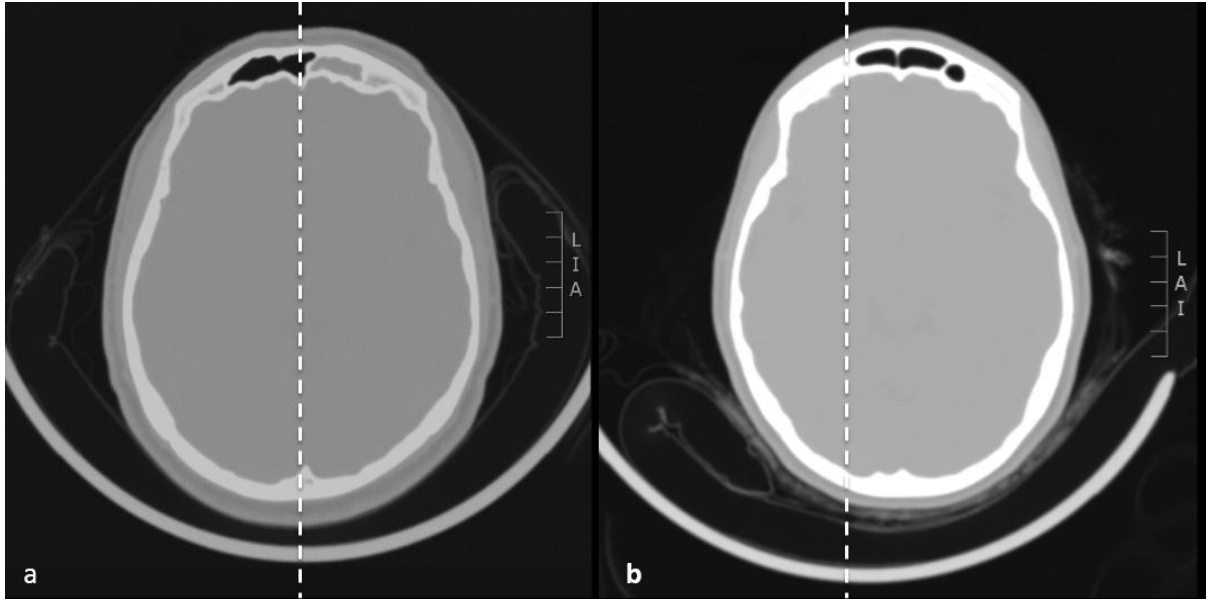


Figure 1. Optimal head centering (a) and sub-optimal head centering (b) during intracranial CT.

Quantitative image analysis

A neuroradiologist certified by the American Board of Radiology and with seven years' experience assessed the images. For all axial reconstructions, 4 mm circular and two regions of interest (ROI) are placed in corresponding white matter (WM) and gray matter (GM) locations (at the level of the basal ganglia) as well as in the pons (these are common areas of stroke prevalence). Signal was defined as CT density in Hounsfield Units (HU), and image noise as standard deviation (SD) of attenuation within a ROI. SNR and CNR were calculated using the following standard equations [20]:

$$SNR = \frac{\text{mean HU of tissue in ROI}}{SD \text{ of HU in ROI}}$$

$$CNR = \frac{\text{mean GM HU} - \text{mean WM HU}}{\sqrt{[(SD \text{ GM HU})^2 + (SD \text{ WM HU})^2]}}$$

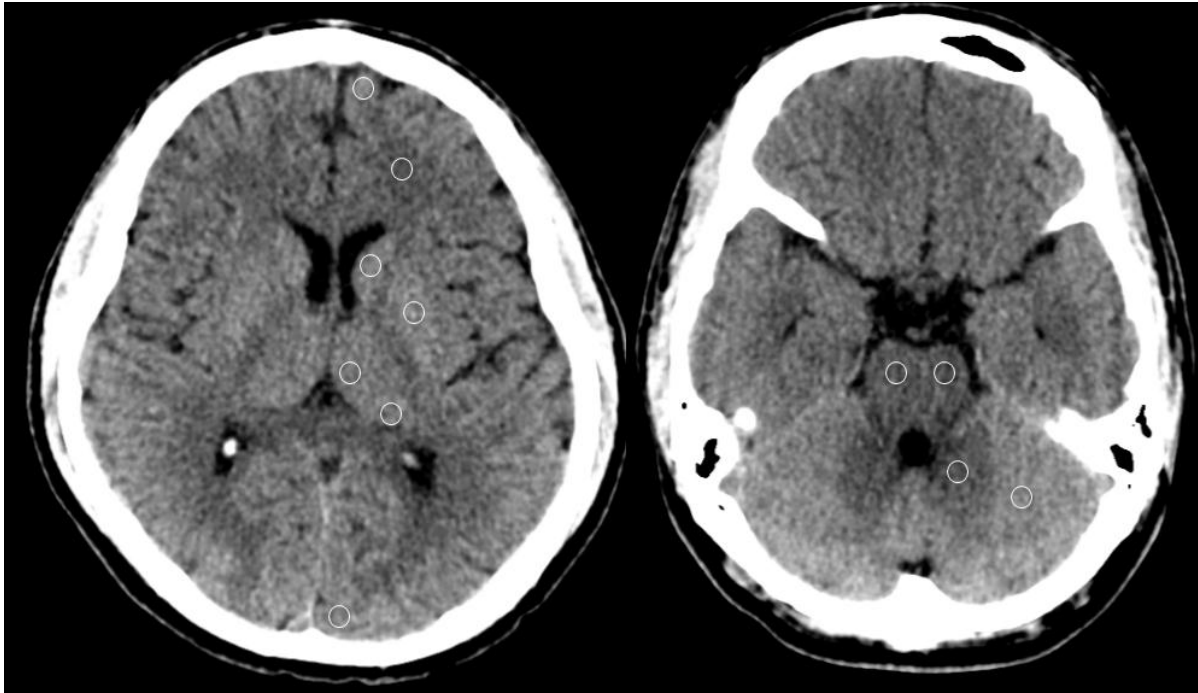


Figure 2. The locations of both gray and white matter: the image on the left demonstrates circular ROI over the frontal, parietal and occipital lobes, and basal ganglia, while the image on the right demonstrates the ROI in the cerebellum and pons.

Qualitative image analysis

Qualitative analysis of images was independently performed by two board-certified, subspecialty certified readers with six and four years of training in neuroradiology, respectively. Prior to the grading of study images, the reading radiologists were trained for consensus regarding our image quality scoring system on 50 routine head CT examinations, which were not included in the study proper. For randomized and anonymous analysis of study patients, subjects or reconstructions were randomly selected by one of our authors and displayed to the readers in a blinded fashion, using two 325 mm × 433 mm screen size monitors with 160 mm × 372 mm image size per individual series. All images were reviewed at a PACS workstation (Centricity; GE Healthcare, Millwake, USA) with use of standard display settings (window level 36, width 80). The relative performance of ICT was assessed using visual grading characteristics (VGC) analysis [21]. VGC is a nonparametric, rank-invariant valid statistical method for image quality evaluation based on visual grading

analyses studies (ordinal ratings). In VGC analysis, plotting the visual grading analyses data of A versus B in a manner similar to that used in ROC analysis assessed the relative performance of pathology detection and image quality. The resulting measure of image quality is the VGC curve, which describes the relationship between the proportions of fulfilled image criteria for the two compared conditions. Subjective image quality will be assessed on axial datasets in terms of noise, grey-white matter differentiation, distinctness of posterior fossa contents, and overall diagnostic acceptability. Noise was graded as 1=very low, 2=low, 3=considerable with preserved diagnostic image quality, and 4=high and causative to non-diagnostic image quality. All other parameters were scored as 1=excellent, 2=good, 3=suboptimal but still diagnostic, and 4=unacceptable and non-diagnostic. Grades for image quality were averaged across both readers for further analysis.

The inter- and intra-observer agreements were calculated using Cohen's kappa analysis. A k value of 0.60–1, 0.41–0.60, 0.21–0.40, and less than 0.20 was considered excellent, moderate, fair, and poor agreement, respectively.

Statistical analysis

Statistical analysis was performed with software (JMP version 6, SAS Institute, Cary, NC; Prism version 4.00, Graph Pad Software, San Diego, CA). A p value of less than 0.05 indicated statistical significance. Unpaired t-test and Chi-square test were used to compare continuous and proportional patient characteristics between the two groups. Comparison of quantitative image quality parameters in axial reconstructions with measurements in standard dose was performed by unpaired t-test. Mann Whitney test was used for comparison of subjective image quality scores. Inter-rater agreement in the assessment of image quality was quantified by weighted kappa statistics [22].

Results

For each protocol, the mean anteroposterior, lateral skull diameters, and cranium circumference demonstrated no significant difference (Table 3).

Table 3: Anatomical correlation between skull parameters and cranial circumference and diameters.

	Group A	Group B	p value
Skull Parameters (mm)			
Anteroposterior Diameter (mm)	174 ± 5.8	173 ± 4.9	> 0.05
Lateral Diameter Head Circumference	136 ± 2.8	138 ± 1.9	> 0.05
	491 ± 11	493 ± 9	> 0.05
	147 ± 21	146 ± 19	> 0.05
Scan Range (mm)			

Note – Data are mean ± standard deviation

Noise measurements

The mean noise was significantly greater in Group A (2.66 ± 0.21) compared to Group B (2.61 ± 0.29) ($p < 0.02$). The mean noise index increased in Group A compared to B when the patient was in the center of the field of view (Table 4).

Table 4: Noise matrix in each section of the image

Noise Location	Group A	Group B	P value
Noise Matrix			
Right top corner	2.61 ± 0.34	2.61 ± 0.31	> 0.05
Right bottom corner	2.65 ± 0.32	2.61 ± 0.29	< 0.02
Left top corner	2.84 ± 0.41	2.62 ± 0.28	< 0.01
Left bottom corner	2.55 ± 0.32	2.62 ± 0.29	> 0.05
Noise Matrix			
Right Side	2.63 ± 0.22	2.61 ± 0.28	< 0.02
Left Side	2.70 ± 0.25	2.62 ± 0.29	< 0.02
Mean Noise Matrix	2.66 ± 0.21	2.61 ± 0.29	< 0.02

Note – Data are mean ± standard deviation

Frontal lobe, occipital lobe and cerebellum

The mean SNR and CNR for WM and GM in the frontal lobe ($p < 0.02$), occipital lobe ($p < 0.04$), and cerebellum ($p < 0.04$) were significantly higher in Group B compared to Group A (Table 5).

Table 5: Anatomical measurements of the frontal lobe, occipital lobe and cerebellum in the brain. The SNR, CNR and Gray-white matter Ratio of the gray and white matter measured in HU. Comparison of the results between Group A (poorly centered) and Group B (incorrectly centered).

Anatomy Location	Group A			Group B			P value
	HU	SNR	CNR	HU	SNR	CNR	
Frontal Lobe							
White Matter	23.65 ±	10.01 ±		21.62 ±	12.31 ±		
Gray Matter	2.46	2.68	8.70 ±	2.46	1.44	15.32 ±	< 0.02
GW Matter	30.90 ±	12.34 ±	1.36	33.36 ±	14.38 ±	1.21	
Ratio	2.59	2.50		2.59	1.33		
Occipital Lobe	1 : 0.77	1 : 0.84		1 : 0.65	1 : 0.85		
White Matter							
Gray Matter	26.82 ±	11.07 ±		28.49 ±	9.07 ±		
GW Matter	2.48	1.98		1.32	1.11		
Ratio	29.41 ±	13.01 ±	10.79 ±	30.44 ±	14.22 ±	14.41 ±	< 0.04
Cerebellum	2.08	2.18	2.11	1.13	3.18	3.09	
White Matter	1 : 1.10	1 : 1.18		1 : 0.94	1 : 0.64		
Gray Matter							
GW Matter	31.03 ±	11.93 ±		31.12 ±	12.47 ±		< 0.04
Ratio	4.46	1.87	12.56 ±	2.39	1.62	14.07 ±	
	39.38 ±	13.21 ±	4.08	38.18 ±	14.39 ±	2.28	
	3.03	2.23		2.11	1.31		
	1 : 0.79	1 : 0.90		1 : 0.82	1 : 0.87		

Note – Data are mean ± standard deviation

Basal ganglia, pons and optic tract

The mean attenuation (HU) of the globus pallidus, caudate nucleus, and optic tract in the basal ganglia demonstrated no difference in attenuation values in each group. The pons demonstrated no significant difference between the left and right side of the pons in each group (Table 6).

Table 6: Anatomical measurements of the basal ganglia, pons and optic tract.

Anatomy Location	HU		HU		P value
	Group A	SNR	Group B	SNR	
Basal Ganglia					
Globus Pallidus	33.28 ±	11.41 ±	33.17 ±	10.33 ±	0.803
Caudate	2.49	1.15	2.46	1.17	0.102
Nucleus	34.89 ±	12.10 ±	26.89 ±	11.19 ±	
Pons	2.07	2.03	2.39	2.33	0.091
Right Side					0.110
Left Side	27.99 ±	9.64 ± 2.48	27.48 ±	9.64 ±	
	2.63	10.77 ±	1.73	2.48	0.683
Optic Tract	29.00 ±	3.18	28.00 ±	11.32 ±	
	2.65		2.65	2.11	
		10.79 ±			
	40.49 ±	1.56	41.10 ±	11.03 ±	
	3.79		1.47	1.86	

Note – Data are mean ± standard deviation

Radiation dose

The mean CTDI_{vol} (specifies the radiation intensity used to perform a specific CT examination) in protocol A (84.58 ± 9.89 mGy) and protocol B (82.38 ± 7.43 mGy), and the mean DLP (amount of radiation = intensity × scan length) in protocol A (1312.03 ± 133.92 mGy·cm) and B (1298.11 ± 130.61 mGy·cm) demonstrated no significant difference between

each protocol (Table 7). The mean effective dose in protocol A (2.76 ± 0.28 mSv) compared to protocol B (2.69 ± 1.18 mSv) was also not significant.

Table 7: Radiation dose values

	Group A	Group B	P value
CTDI _{vol}	84.58 ± 9.89	82.38 ± 7.43	0.092
DLP (mGy x cm)	1312.03 ± 133.92	$1298.11 \pm$ 130.61	0.092
Effective Dose (mSv)	2.76 ± 0.28	2.69 ± 1.18	0.092

Note – Data are mean \pm standard deviation

Qualitative image analysis

The VGC graphs are shown in Figures 3a and 3b. Each reader's results were graphed separately for each group. When a preference is shown towards one group the curve is convex to that group's axis. The graphs clearly show that when the head is centered correctly and the GWM interface was assessed for image quality, the preference is for Group B over Group A for both readers.

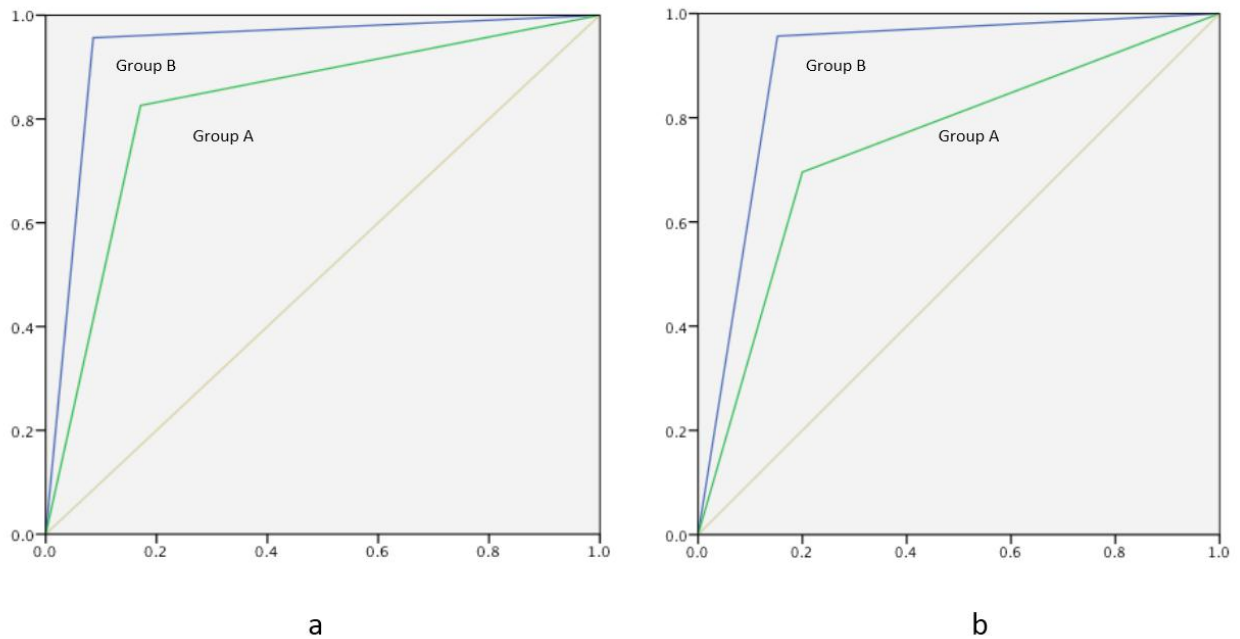


Figure 3. VGC curve. Graph (a) represents reader 1 and (b) reader 2. Each reader demonstrated increased image quality in group B compared to A.

The kappa values of the independent ratings of GWM image quality by the two independent radiologists ranged from 0.62 to 0.81 (mean 0.74), indicating substantial to almost perfect agreement.

Discussion

The number of CT examinations continues to rise and studies highlight a worrisome risk of lifetime cancer from medical radiation exposure. Consequently, there is a quest for powerful tools to ultimately limit the per scan radiation dose. Until recently, the efficiency of all dose-reduction strategies was drastically limited by inherent characteristics of the standard reconstruction algorithm, filtered back projection. As the latter contains a trade-off between image sharpness and noise, significant reduction of standard dose is invariably associated with loss of image quality. While mild increase of noise may not limit diagnostic accuracy in many conventional CT applications, classic challenges in neuroradiology such as detection of ischemia, edema, or traces of intracranial hemorrhage leave little room for compromise. Our

study demonstrated that whilst we were below the radiation dose threshold, the importance of GWM ratio is proven to be a stronger quantitative measurement than qualitative indications such as VGC and Kappa analyses alone.

Poor patient centering occurs in two ways. The first occurs when patients present to the radiology department with altered neurological conditions such as Parkinson's disease, severe head trauma, and altered mental status, resulting in uncooperative patients. Secondly, when radiographers face extreme workloads and time constraints, the radiographer-patient interaction time is reduced resulting in poor patient education and increased chance of movement. Proper patient centering results in optimal automatic exposure control and image quality. However, with off-center positioning, reduced uniformity in image quality (both quantitative and qualitative) may obscure anatomical details (Figures 4a and b). Therefore, to maintain image quality, clear patient education, effective head and chin strapping techniques on the head holder, and changing exposure factors such as kVp, mAs, and pitches increases the speed of the examination without increasing radiation dose and its effects on the GWM interface [23]. Our study demonstrated no significant difference between delivered radiation doses, however, there was increased separation between the GMW interfaces.

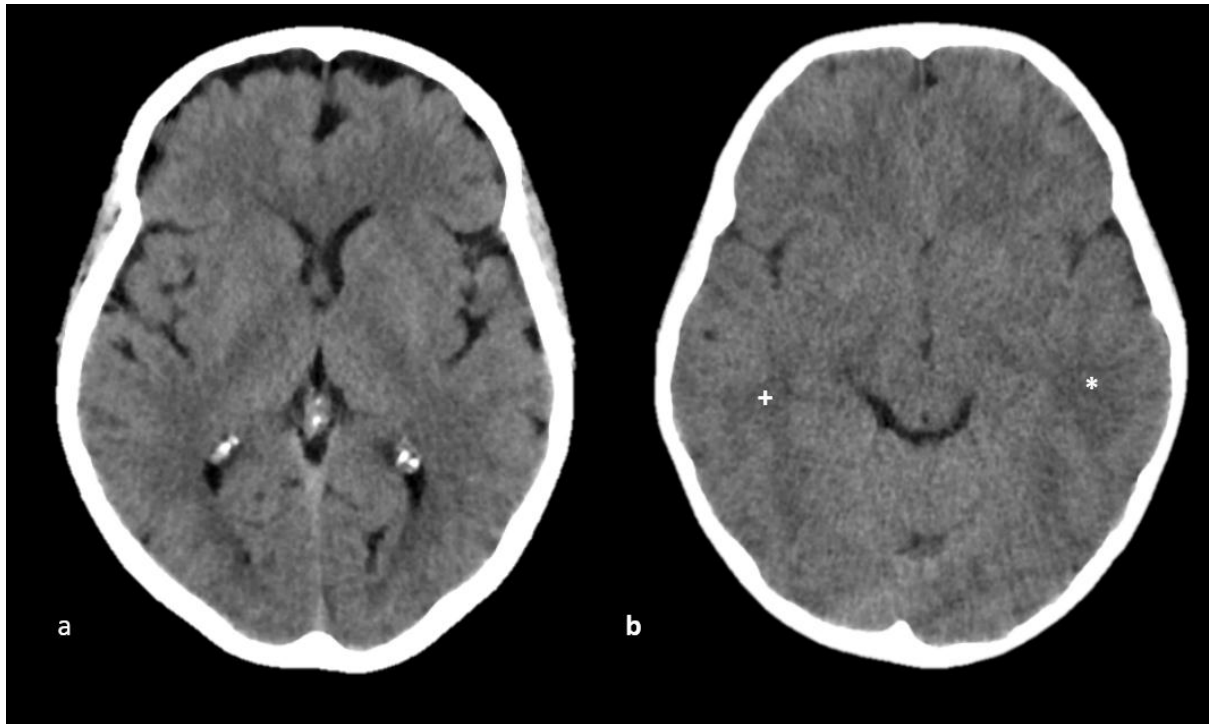


Figure 4: Optimal head centering with uniform gray and white matter in each side of the neural hemispheres (a), while, sub-optimal head centering demonstrated increased white matter density in the left hemisphere (*) compared to the right (+) (b) during intracranial CT.

The human visual system requires a certain level of contrast difference between structures to record a perceptual change. By enhancing and reducing the brightness of the GM and WM systems, respectively, this separation increases the GWM ratio with optimal centering, which was demonstrated in the current study. Accordingly, the quantitative and qualitative findings are supported by our clinical (VGC and Kappa) data with Group B ($p < 0.02$) demonstrating significant increase in qualitative and quantitative image quality when the head was centered in the center of the field of view.

Radiologists are known to critique brain CT scans by ensuring there is optimal separation between the gray and white matter [7–12, 15, 16]. In order to achieve the optimal differences, low noise and high signal are preferred to detect low-contrast resolution structures and pathological processes. Within a DRL, the amount of noise is directly proportional to the amount of radiation dose which is emitted. However, our study

demonstrated that the optimal separation between the GWM interfaces was well below the DRL for intracranial CT with the CNR being the most accurate measurement in measuring optimal image quality between the gray and white matter in Group B ($p < 0.04$).

There are limitations to our study. First, we did not perform a comparison between filtered back projection and iterative reconstruction on the same group of patients because it would be inappropriate to expose children and adults to unnecessary radiation; rather, we preferred to compare the means of different patient groups. Second, as the quality of the examination was the focus of the study, we did not compare all of the CT findings and assess the diagnostic accuracy.

Conclusion

In conclusion, we found that correct patient centering increases the contrast and signal in both gray and white matter on the right and left hemispheres of the brain during intracranial computed tomography.

References

1. Shuryak I, Lubin JH, Brenner DJ. Potential for adult-based epidemiological studies to characterize overall cancer risks associated with a lifetime of CT scans. *Radiat Res.* 2014;181(6):584-91.
2. Brenner DJ, Hall EJ. Cancer risks from CT scans: now we have data, what next? *Radiology.* 2012;265(2):330-1.
3. Brenner DJ, Shuryak I. Ten years of follow-up is not long enough to assess lifetime cancer risks caused by computed tomography scans in a young population. *J Clin Oncol.* 2011;29(30):4062; author reply
4. The 2007 Recommendations of the International Commission on Radiological Protection. ICRP publication 103. *Ann ICRP.* 2007;37(2-4):1-332.
5. Strauss KJ. Developing patient-specific dose protocols for a CT scanner and exam using diagnostic reference levels. *Pediatr Radiol.* 2014;44 Suppl 3:479-88.
6. Schafer S, Alejandre-Lafont E, Schmidt T, Gizewski ER, Fiebich M, Krombach GA. Dose management for X-ray and CT: systematic comparison of exposition values from two institutes to diagnostic reference levels and use of results for optimisation of exposition. *Rofo.* 2014;186(8):785-94.
7. Moorin RE, Gibson DA, Forsyth RK, Bulsara MK, Holman CD. Evaluating data capture methods for the establishment of diagnostic reference levels in CT scanning. *Eur J Radiol.* 2014;83(2):329-37.
8. Leithner R, Homolka P. A quantitative comparison of data evaluation methods to derive diagnostic reference levels for CT from a dosimetric survey: correlation analysis compared to simple evaluation strategies. *Phys Med.* 2013;29(5):470-7.
9. Foley SJ, McEntee MF, Rainford LA. Establishment of CT diagnostic reference levels in Ireland. *Br J Radiol.* 2012;85(1018):1390-7.
10. McCollough C, Branham T, Herlihy V, Bhargavan M, Robbins L, Bush K, et al. Diagnostic reference levels from the ACR CT Accreditation Program. *J Am Coll Radiol.* 2011;8(11):795-803.
11. Jarvinen H, Merimaa K, Seuri R, Tyrvaainen E, Perhoma M, Savikurki-Heikkila P, et al. Patient doses in paediatric CT: feasibility of setting diagnostic reference levels. *Radiat Prot Dosimetry.* 2011;147(1-2):142-6.
12. Treier R, Aroua A, Verdun FR, Samara E, Stuessi A, Trueb PR. Patient doses in CT examinations in Switzerland: implementation of national diagnostic reference levels. *Radiat Prot Dosimetry.* 2010;142(2-4):244-54.
13. Verdun FR, Gutierrez D, Vader JP, Aroua A, Alamo-Maestre LT, Bochud F, et al. CT radiation dose in children: a survey to establish age-based diagnostic reference levels in Switzerland. *Eur Radiol.* 2008;18(9):1980-6.
14. Toth T, Ge Z, Daly MP. The influence of patient centering on CT dose and image noise. *Med Phys.* 2007;34(7):3093-101.
15. Tsapaki V, Aldrich JE, Sharma R, Staniszewska MA, Krisanachinda A, Rehani M, et al. Dose reduction in CT while maintaining diagnostic confidence: diagnostic reference levels at routine head, chest, and abdominal CT--IAEA-coordinated research project. *Radiology.* 2006;240(3):828-34.
16. Heliou R, Normandeau L, Beaudoin G. Towards dose reduction in CT: patient radiation dose assessment for CT examinations at university health center in Canada and comparison with national diagnostic reference levels. *Radiat Prot Dosimetry.* 2012;148(2):202-10.

17. Paolicchi F, Faggioni L, Bastiani L, Molinaro S, Puglioli M, Caramella D, et al. Optimizing the Balance Between Radiation Dose and Image Quality in Pediatric Head CT: Findings Before and After Intensive Radiologic Staff Training. *American Journal of Roentgenology*. 2014;202(6):1309-15.
18. Goo HW. CT radiation dose optimization and estimation: an update for radiologists. *Korean J Radiol*. 2012;13(1):1-11.
19. Christner JA, Kofler JM, McCollough CH. Estimating effective dose for CT using dose-length product compared with using organ doses: consequences of adopting International Commission on Radiological Protection publication 103 or dual-energy scanning. *AJR Am J Roentgenol*. 2010;194(4):881-9.
20. Mullins ME, Lev MH, Bove P, O'Reilly CE, Saini S, Rhea JT, et al. Comparison of Image Quality Between Conventional and Low-Dose Nonenhanced Head CT. *American Journal of Neuroradiology*. 2004;25(4):533-8.
21. Bath M, Mansson LG. Visual grading characteristics (VGC) analysis: a non-parametric rank-invariant statistical method for image quality evaluation. *Br J Radiol*. 2007;80(951):169-76.
22. Viera AJ, Garrett JM. Understanding interobserver agreement: the kappa statistic. *Fam Med*. 2005;37(5):360-3.
23. Trattner S, Pearson GD, Chin C, Cody DD, Gupta R, Hess CP, et al. Standardization and optimization of CT protocols to achieve low dose. *J Am Coll Radiol*. 2014;11(3):271-8.